

MITIGATION OF POWER QUALITY PROBLEMS IN STEEL PLANTS USING STATIC SYNCHRONOUS COMPENSATOR

YACINE DJEGHADER^{1,*}, CHOAYB BOUSNOUBRA¹, SELMA ALLELE¹

Keywords: Electrical arc furnace (EAF); Flicker; Fuzzy logic controller (FLC); Harmonics; Power quality; Static synchronous compensator (STATCOM); Steel plant.

This paper focuses on mitigating various power quality issues from electric arc furnaces (EAF) in steel plants, including voltage flicker, sag, swell, and harmonics. Arc furnaces are recognized as one of the industry's most nonlinear electrically polluting loads. The proposed solution in this article to address all power quality issues caused by EAF is implementing a flexible power supply strategy known as a static synchronous compensator (STATCOM) for injecting reactive energy into the electrical grid. In this study, an experimental model of EAF is utilized based on real measurements of the variation of arc resistance and arc reactance during the melting phase. The pulse width modulation (PWM) technique is employed for current tracking feedback control to generate the required reactive current. A fuzzy logic controller (FLC) is employed for the DC bus.

1. INTRODUCTION

The power quality field has become very important in recent years due to the development of power electronics equipment and its application in electric power systems [1]. The electric arc furnace (EAF) is a crucial piece of equipment utilized in steel production, employing heat generated by short-circuit currents. Due to the inherent characteristics of the electric arc, which include non-linearity, instability, and asymmetry, the EAF is recognized as a significant source of power quality issues. These problems encompass a range of issues, such as voltage fluctuations, sags, swells, unbalanced voltages across the three phases, and the generation of current harmonics and inter-harmonics [2]. Voltage flicker and current harmonics stand out as some of the most challenging power quality issues arising from the operation of electric arc furnaces. Voltage flicker primarily stems from significant and rapid changes in industrial loads, leading to power fluctuations and light intensity variations [3,4]. These fluctuations can not only disrupt the stability of the power grid but also affect the performance of sensitive equipment connected to it.

Similarly, current harmonics, generated due to the non-linear behavior of electric arc furnaces, can distort voltage and current waveforms, leading to increased losses, overheating of equipment, and interference with communication systems. Addressing these issues is crucial for maintaining a stable and reliable power supply in industrial settings [5]. Hence, we should have an effective solution to mitigate this power quality problem. When we have good power quality, the production process becomes more important. For this reason, it is essential to mitigate these problems by delivering energy without degradation and in compliance with international standards. In this paper, we investigate, design, and performance evaluation of STATCOM for enhancing power quality in steel plants, utilizing the MATLAB environment (Simulink). The method injects reactive energy into the electrical grid through STATCOM, employing instantaneous reactive current detection and fuzzy logic control.

2. ELECTRIC ARC FURNACE MODELING

In recent years, numerous models have been proposed, particularly within mathematical modeling, which employs nonlinear equations to capture the stochastic behavior

inherent in the operation of EAF [6]. However, it is crucial to acknowledge that these models, though significant in their attempts, remain inherently approximate. They need to accurately portray the intricate workings of an EAF across various operational stages and often overlook the influence of numerous variable factors.

Despite these limitations, leveraging experimental data about the fluctuation of resistance and reactance of the electrical arc [7] offers a promising avenue for obtaining deeper insights into EAF dynamics. It is noteworthy to highlight a particular model proposed in [7,8] that stands out for its comprehensive examination of waveforms, specifically focusing on the variations observed in the parameters of resistance (R_{arc}) and reactance (X_{arc}).

This model not only underscores the significance of these waveforms but also encapsulates a multifaceted understanding of EAF behavior, thereby offering valuable insights for further analysis and refinement.

This article uses the model proposed in [7–9] based on:

$$R_{arc} = A_R(v)e^{\alpha(v)d}, \quad (1)$$

$$A_R = \frac{[0.7(V-210^2)+1.7]}{50^2} 10^{-3}, \quad (2)$$

$$\alpha = 0.097e^{0.011(90-V)} - \frac{1.7}{(V-112)^2+80} + \frac{100}{(V-360)^2+50}, \quad (3)$$

$$X_{arc} = A_X(v)d^2 + B_X(v), \quad (4)$$

$$A_X = 1.05 \times 10^{-3} e^{0.075(90-V)}, \quad (5)$$

$$B_X = \frac{3.14}{153} - 3 \times 10^{-3} \cdot e^{0.075(90-V)}, \quad (6)$$

where d is the distance between the electrode and the scrap.

This experimental model only applies to the arc furnace at steel plants in Annaba, Algeria. The parameters of this furnace are presented in Table 1.

Table 1
Parameters of electric arc furnaces studied

| | |
|-----------------------------------|--|
| Power Transformer | 12.5 MVA |
| The reactance (short circuit) | 2.9 mΩ |
| Electrode current (maximum) | 30.84 kA |
| Secondary voltage range | 90 - 112- 149- 160- 174- 190- 210- 234- 265 V |
| Number of secondary voltage range | 9 |
| Primary Nominal voltage: | 63 kV |
| STATCOM | ± 3 Mvar |

¹ University of Mohamed-Cherif Messaadia, LEER Laboratory Souk Ahras, Algeria

Emails: yacine.djeghader@univ-soukahras.dz (correspondence), c.bousnoubra@univ-soukahras.dz, allaleselma@gmail.com

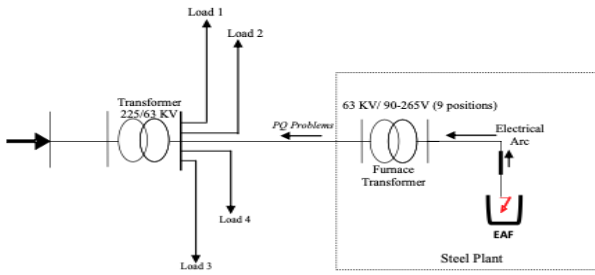


Fig. 1 – Single line diagram of electric arc furnace studied.

3. EXPERIMENTAL PART

We have employed empirical data from operational measurements of the arc furnace during its melting phase, as documented in references [7–9]. Within our analysis, we have meticulously recorded the harmonic currents and total harmonic distortion of current (THDI), noted in Table 2.

Table 2
Harmonics values and THDI₁ measurements

| | | | | | |
|----------------|---------|-----------------|--------|-------------------------|---------------|
| H ₂ | 14.45 % | H ₇ | 3.59 % | H ₁₂ | 0.71 % |
| H ₃ | 32.62 % | H ₈ | 2.22 % | H ₁₃ | 2.28 % |
| H ₄ | 5.1 % | H ₉ | 3.19 % | H ₁₄ | 1.69 % |
| H ₅ | 10.04 % | H ₁₀ | 1.69 % | H ₁₅ | 1.6 % |
| H ₆ | 6.56 % | H ₁₁ | 1.34 % | THDI₁ | 38.4 % |

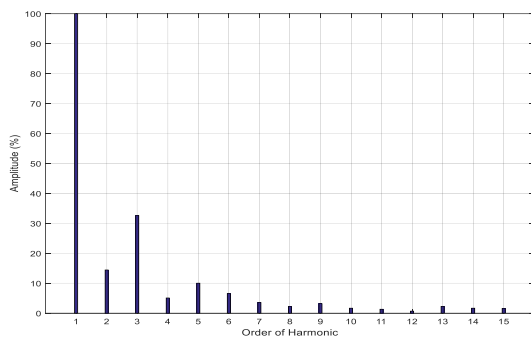


Fig. 2 – Harmonic spectrum of current.

Based on the values of the current harmonics (Table 2) and the parameters of the studied arc furnace (Table 1), we can plot the current absorbed by the furnace as follows:

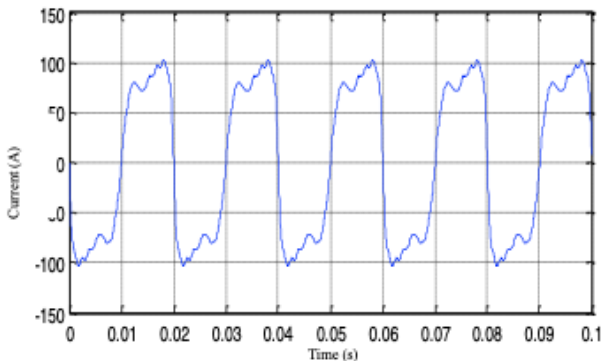


Fig. 3 – Arc current waveform.

We can calculate the voltage fluctuation at PCC using

$$\frac{\Delta V}{V_n} = \frac{V_{max} - V_{min}}{V_n} \cdot 100 = \frac{1.02 - 0.95}{1.0} \cdot 100 = 7\%. \quad (7)$$

and the rate of voltage sag (Dip) at PCC using

$$\frac{\Delta V}{V_n} = \frac{1.02 - 0.6}{1.0} \cdot 100\% = 42\%, \quad (8)$$

V_{max} is the maximum voltage at PCC, V_{min} is the minimum voltage at PCC, and V_n is the nominal voltage.

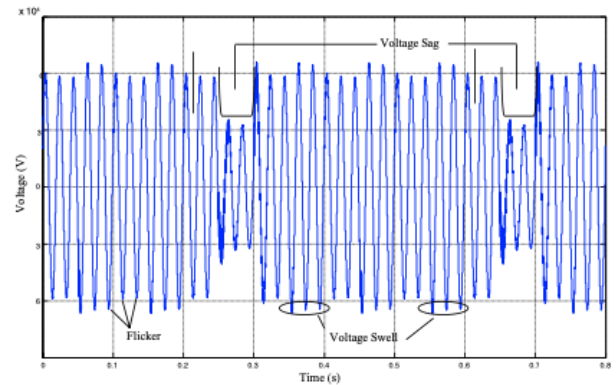


Fig. 4 – The voltage waveform at PCC (63 kV).

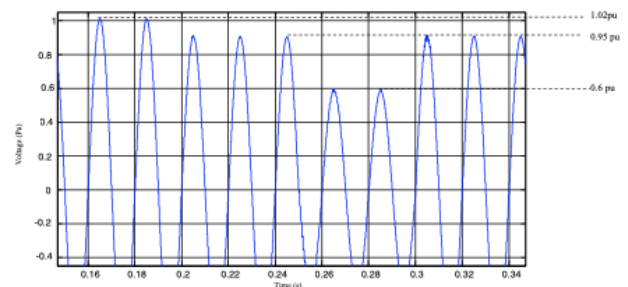


Fig 5 – Waveform of voltage at PCC in PU.

4. STATIC SYNCHRONOUS COMPENSATOR (STATCOM)

STATCOM is a member of the family of devices known as Flexible Alternating Compensators (FACTS), renowned for their ability to dynamically regulate voltage and reactive power in power systems. Typically, STATCOMs are connected in parallel via a reactance, ensuring seamless integration into the electrical grid while providing essential reactive power support and voltage [10]. The principle is to control the output voltage of the STATCOM, the purpose of which is that the desired current can be forced to flow through the reactor link. The basic configuration of Fig. 9 shows that STATCOM is installed parallel to the electrical grid network via a transformer. The operating principle involves adjusting the phase and amplitude of the output voltage while simultaneously controlling the output current of STATCOM. Its purpose is to either instantly absorb or generate the necessary reactive current to compensate for the reactive current generated by the polluting load [10,11].

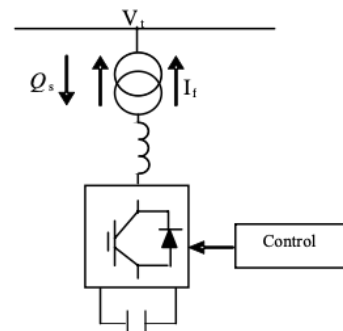


Fig. 6 – The basic circuit of STATCOM.

4.1. DETECTION AND CONTROL OF INSTANTANEOUS REACTIVE CURRENT

The instantaneous reactive current can be obtained by relying on the instantaneous reactive power theory, adopting the instantaneous active power p and the instantaneous reactive power q as the starting condition [12]. When the system voltage remains constant, controlling the reactive current is the same as controlling the reactive power. The schematic diagram in Fig. 7 shows the method followed. Here v_a, v_b and v_c are instantaneous on (abc) system, and i_a, i_b , and i_c are instantaneous on (abc) system.

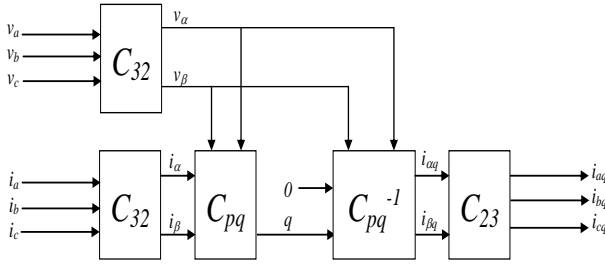


Fig. 7 – Instantaneous reactive current detection schematic.

The instantaneous voltages and currents on the (abc) system can be transformed into the ($\alpha\beta$) system v_α, v_β and the i_α, i_β by using (eq. (12) and (13))

$$\begin{bmatrix} v_\alpha \\ v_\beta \end{bmatrix} = C_{32} \cdot \begin{bmatrix} v_a \\ v_b \\ v_c \end{bmatrix}, \quad (12)$$

$$\begin{bmatrix} i_\alpha \\ i_\beta \end{bmatrix} = C_{32} \cdot \begin{bmatrix} i_a \\ i_b \\ i_c \end{bmatrix}, \quad (13)$$

$$C_{32} = \sqrt{\frac{2}{3}} \cdot \begin{bmatrix} 1 & -\frac{1}{2} & -\frac{1}{2} \\ 0 & \frac{\sqrt{3}}{2} & -\frac{\sqrt{3}}{2} \end{bmatrix}. \quad (14)$$

The following relationship calculates the three-phase instantaneous real power

$$p = v_a i_a + v_b i_b + v_c i_c. \quad (15)$$

Therefore, the instantaneous power can be rewritten, as shown in equation 16

$$\begin{bmatrix} p \\ q \end{bmatrix} = C_{pq} \cdot \begin{bmatrix} i_\alpha \\ i_\beta \end{bmatrix}. \quad (16)$$

The currents are calculated as follows:

$$\begin{bmatrix} i_\alpha \\ i_\beta \end{bmatrix} = C_{pq}^{-1} \cdot \begin{bmatrix} p \\ q \end{bmatrix}, \quad (17)$$

$$C_{pq} = \begin{bmatrix} v_\alpha & v_\beta \\ -v_\beta & v_\alpha \end{bmatrix}, \quad (18)$$

$$C_{pq}^{-1} = \begin{bmatrix} v_\alpha & v_\beta \\ -v_\beta & v_\alpha \end{bmatrix}^{-1}. \quad (19)$$

Knowing that our compensator will only compensate reactive power, so the active power will always be set to zero. The necessary reactive power is defined in opposite vectors whose purpose is to cancel the reactive part of the line current

$$\begin{bmatrix} i_{aq} \\ i_{bq} \\ i_{cq} \end{bmatrix} = C_{32} \cdot C_{aq} \cdot \begin{bmatrix} 0 \\ q \end{bmatrix}, \quad (20)$$

where i_{aq}, i_{bq} and i_{cq} are instantaneous reactive currents on abc system and

$$C_{32} = \sqrt{\frac{2}{3}} \cdot \begin{bmatrix} 1 & 0 \\ -\frac{1}{2} & \frac{\sqrt{3}}{2} \\ -\frac{1}{2} & -\frac{\sqrt{3}}{2} \end{bmatrix}. \quad (21)$$

4.2. FUZZY CONTROL APPLICATION

The condensation of DC voltage is compared with the desired reference value. So, we can write the voltage error as follows ($e = V_{dc-ref} - V_{dc}$). The error (e) and its derivation (de/dt) are used as inputs for the FLC process [13,14].

The FLC is characterized by five fuzzy sets in linguistic variables, such as negative (N), big negative (BN), zero (Z), positive (P), and big positive (BP) for each input and output variable. A triangular membership function is used for its simplicity. For implication, we use a Mamdani-type min-operator. The phase of defuzzification uses the centroid method. The principal block diagram of the FLC with two inputs (error (e) and its derivative (de/dt)) is illustrated in Fig. 8.

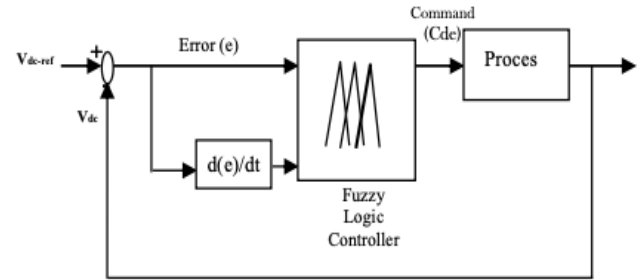


Fig. 8 – Fuzzy logic controller (FLC) scheme.

The FLC technique decomposes in three steps: fuzzification, fuzzy inference mechanism (knowledge base), and defuzzification.

Fuzzification is converting a numerical value e into a linguistic value.

Rule Elevator. The linguistic variables used by FLC as a control gain. The principal's operations of FLC require AND (\cap), OR (\cup) and NOT (\sim) for evaluation of fuzzy set rules.

Defuzzification is the return operation, *i.e.*, converting the linguistic variable (value) into a numeric variable (value).

Database stores the definition of the triangular membership function for the fuzzifier and defuzzifier.

Rule Base stores the linguistic control rules required by the rule evaluator.

Our controller has twenty-five rules, presented in Table 3, Fig. 9.

Table 3
FLC rules

| C_{de} | | de/dt | | | | |
|----------|----|---------|----|----|----|----|
| | | BN | N | Z | P | BP |
| e | BN | BN | BN | BN | N | Z |
| | N | BN | N | N | Z | P |
| | Z | BN | N | Z | P | BP |
| | P | N | Z | P | P | BP |
| | BP | Z | P | BP | BP | BP |

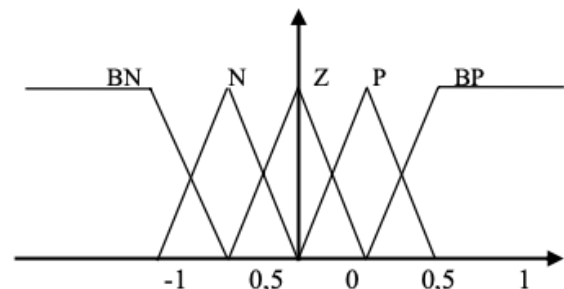


Fig. 9 – Membership functions of FLC.

5. SIMULATION PART

The circuit illustrated in Figs. 10 and 11 serves as a pivotal component for controlling the STATCOM and detecting the instantaneous reactive current (I_{ref}), which is imperative for compensating for the requisite reactive power.

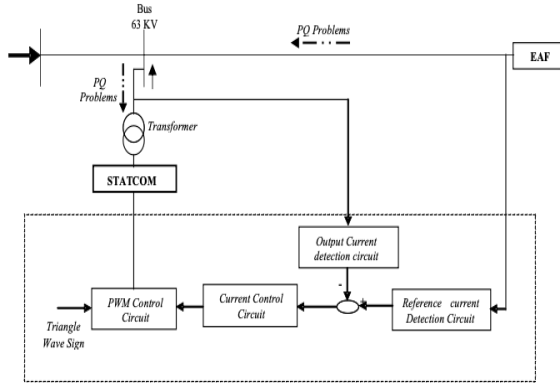


Fig. 10 – Schematic of the studied system.

Adopting PWM control for the converter is particularly noteworthy, as it is pivotal in augmenting electrical quality. This technique significantly contributes to the overarching improvement of power quality standards.

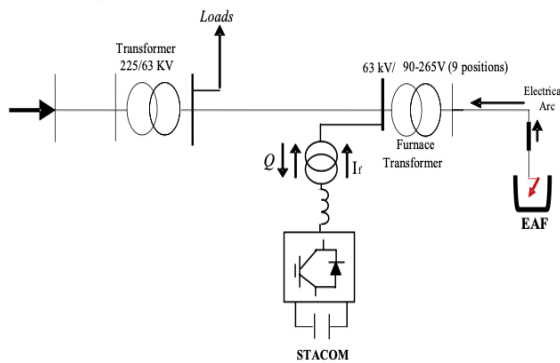


Fig. 11 – The basic control of the STATCOM.

In Figs. 12 and 13, we present the voltage waveform at the level of the output of the furnace's transformer, 63 kV.

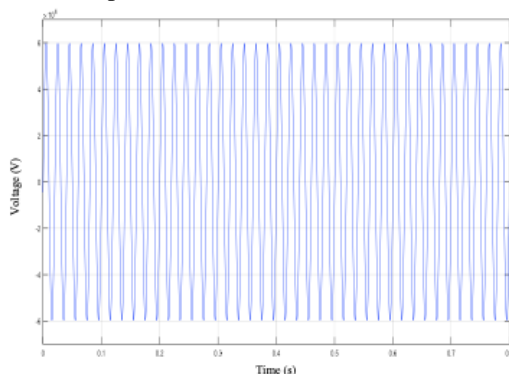


Fig. 12 – Voltage waveform after using SATCOM.

The rate of voltage flicker:

$$\frac{\Delta V}{V_n} = \frac{1.0 - 0.987}{1.0} 100 \% = 1.3 \% \quad (22)$$

According to the harmonic spectrum presented in Fig. 14 and the percentage of harmonic currents and the total harmonic distortion rate (Table 4).

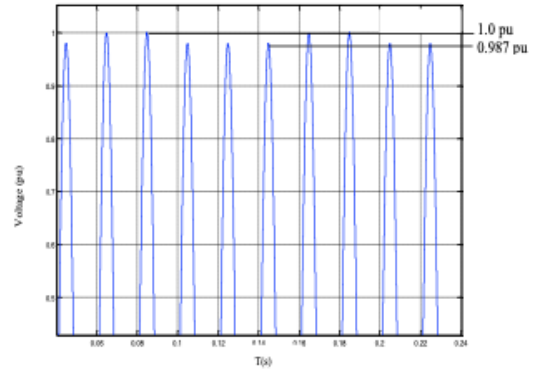


Fig. 13 – Voltage waveform after using STATCOM in (PU).

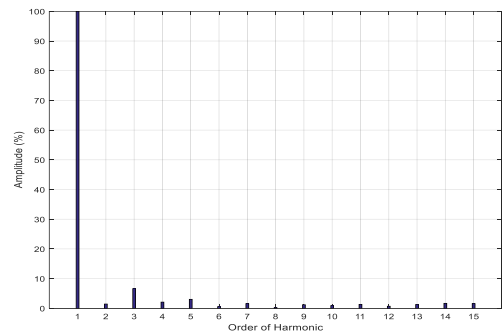


Fig. 14 – Harmonic spectrum of current after using STATCOM.

Table 4

| Harmonics values and THD ₁ with STATCOM | | | | | |
|--|--------|-----------------|--------|------------------------|---------------|
| H ₂ | 0.45 % | H ₇ | 1.50 % | H ₁₂ | 0.31 % |
| H ₃ | 3.55 % | H ₈ | 0.25 % | H ₁₃ | 1.11 % |
| H ₄ | 0.10 % | H ₉ | 1.10 % | H ₁₄ | 0.25 % |
| H ₅ | 2.04 % | H ₁₀ | 0.90 % | H ₁₅ | 0.40 % |
| H ₆ | 0.25 % | H ₁₁ | 1.12 % | THD₁ | 4.93 % |

6. DISCUSSION

After installing the STATCOM, observations reveal the mitigation of voltage disturbances, including voltage sags, swells, and fluctuations, as illustrated in Fig. 12. This phenomenon underscores the pivotal role of STATCOM in reactive power compensation, facilitated by implementing efficient techniques. Consequently, the resultant voltage flicker rate is measured at 1.3%, as depicted in Fig. 13. Notably, this value is well below the threshold of 2% stipulated by the Chinese national standard (GB12326-2000), indicating compliance with regulatory benchmarks. Furthermore, this achievement underscores the mitigation strategies' efficacy in enhancing power quality and ensuring operational reliability within the electrical network.

Table 4 shows that all parameters adhere to the stringent criteria outlined in the IEEE 512 standard, with a maximum allowable threshold of less than 5%. This observation underscores the efficacy of the implemented measures in mitigating harmonic distortions within the electrical system.

7. CONCLUSION

This article introduces STATCOM as a modern, universal, and adaptable solution for addressing the array of power quality issues arising during the operation of electric arc furnaces. Initially, we employ an experimental model based on a study of variations of resistance and reactance of the electric arc, as well as harmonic current generated in the

melting phase, to facilitate the assessment of degradation levels. Subsequently, we propose a comprehensive solution to rectify diverse electrical disturbances. Leveraging the Simulink tool of MATLAB, we meticulously develop and validate our proposed system. Simulation results affirm the effectiveness of the employed strategy in mitigating power quality problem concerns, notably voltage flicker, voltage sag, and harmonics.

Received on 14 April 2023

REFERENCES

1. N. Daou, H.F. Fassi, N. Ababssi, Y. Djeghader, *Minimum variance control of active filter for reduction of harmonics*, Rev. Roum. Sci. Techn. – Électrotechn. et Énerg., **6**, 4, pp. 391–395 (2019).
2. H. Samet, S. Gashtasbi, N. Tashakor, T. Ghanbari, *Improvement of reactive power calculation in electric arc furnaces utilising Kalman filter*, Science Measurement & Technology IET, **11**, 3, pp. 241–248 (2017).
3. R. Hooshmand, M. Banejad, M-T. Esfahani, *A new time domain model for electric arc furnace*, Journal of Electrical Engineering, **59**, 4, 195–202 (2008).
4. G.C. Lazaroiu, D. Zaninelli, *A control system for DC arc furnaces for power quality improvements*, Electric Power Systems Research, **80**, 12, pp. 1498–1505, 2010.
5. Y. Varetzky, V. Konoval, M. Sehedra, O. Pastuh, *Studying voltage fluctuations in microgrid with hybrid renewable energy system*, Proc. IEEE 6th Int. Conf. on Energy Smart Systems, pp. 239–242 (2019).
6. H. Samet, A. Mojallal, T. Ghanbari, *Employing grey system model for prediction of electric arc furnace reactive power to improve compensator performance*, Przegląd Elektrotechniczny, **89**, pp. 110–115 (2013).
7. H. Labar, Y. Djeghader, K. Bounaya, M-S. Kelaiaia, *Improvement of electrical arc furnace operation with an appropriate model*, Journal Energy, Elsevier, **34**, pp. 1207–1214 (2009).
8. Y. Djeghader, H. Labar, K. Bounaya, *Modelling and parametrical approximation of an electric arc furnace steelmaking*, Journal of Electrical Engineering (JEE), **9**, 3, pp. 25–30 (2009).
9. Y. Djeghader, H. Labar, K. Bounaya, *Analysis of harmonics generated by different structures of a DC EAF*, International Review of Modelling and Simulations (IREMOS), **1**, 1, pp. 173–177 (2008).
10. S. Arockiaraj, B.V. Manikandan A. Bhuvanesh, *Fuzzy logic controlled STATCOM with a series compensated transmission line analysis*, Rev. Roum. Sci. Techn. – Électrotechn. et Énerg., **68**, 3, pp. 307–312 (2023).
11. M. Gavrilas, R. Toma, *Flexible alternating current transmission system optimisation in the context of large disturbance voltage stability*, Rev. Roum. Sci. Techn. – Électrotechn. et Énerg., **66**, 1, pp. 21–26 (2021).
12. H. Akagi, Y. Kanazawa, A. Nabae, *Instantaneous reactive power compensators comprising switching devices without energy storage components*, IEEE Trans. on Industry Applications, **20**, 3, pp. 625–630 (1984).
13. S. Saad, L. Zellouma, *Fuzzy logic controller for three-level shunt active filter compensating harmonics and reactive power*, Elsevier, Electric Power Systems Research, **79**, pp. 1337–1341 (2009).
14. N. Zidane, S.L. Belaid, *A new fuzzy logic solution for energy management of hybrid photovoltaic /battery/hydrogen system*, Rev. Roum. Sci. Techn. – Électrotechn. et Énerg., **67**, 3, pp. 21–26 (2022).